Stanford Exploration Project, Report 111, June 9, 2002, pages 47–59

Converted wave dip moveout

Daniel Rosales[1]

ABSTRACT

Dip moveout (DMO) introduces a dip-dependent correction for a more appropiate transformation of prestack data into zero-offset data. Converted wave DMO has been discussed in the literature by severeal authors. Log-stretch *f-k* PS-DMO has been recently introduced in the literature. At the moment, however, this PS-DMO operator presents problems of handling amplitudes properly. A PP-DMO in this domain that accurately handle amplitudes already exists. Therefore, it is important to extend such operator for PS data. This new operator for converted waves is presented in this paper. I show impulse responses and real data results using the new PS-DMO operator.

INTRODUCTION

The problem of sorting, NMO correction and stacking for PS data has been widely addressed in the past (Tessmer and Behle, 1988; Iverson et al., 1989). The solutions presented in these works apply a lateral shift to the trace midpoints, such that the new trace position corresponds with the lateral position of the conversion point. Usually, this correction does not incorporate the effects of the reflector depth and dip.

In order to incorporate the dip effect, Huub Den Rooijen (1991) achieves the transformation from CMP-sorted data to CCP-sorted data using a dip moveout operator. In a similar way to the PP-DMO, PS-DMO may reduce the problem of reflection point dispersal due to dip without knowledge of the reflector geometry. Most of the existing PS-DMO operators present errors due to truncation of power series and/or second order approximations (Xu et al., 2001). Xu et al. (2001) show a fast converted dip moveout operator in the *f-k* domain which partially alleviates approximation errors.

Harrison (1990) presents the zero-offset mapping equation for the PS-DMO operator, applying an integral-summation approach in order to implement his PS-DMO operator.

Xu et al. (2001) present a log-stretch *f-k* PS-DMO operator. His operator correctly handles the kinematics, but doesn't handle amplitudes properly. Here, I present a review of the PS-DMO operator, implement the operator described by Xu et al. (2001) and extend it to handle the amplitudes properly.

[1]**email:** daniel@sep.stanford.edu

KINEMATICS OF PS-DMO

The downgoing and upgoing waves travel at different velocities for converted wave data. This difference makes the kinematics more complicated than that of single mode data.

The kinematics of PS-DMO have been widely discussed in the literature. Harrison (1990) is the first one to derive the zero-offset mapping equation for converted waves. He uses an integral-summation approach, similar to Deregowski and Rocca (1981) in order to apply DMO to converted waves data. He also applies the PS zero-offset mapping and the adjoint of his operator in order to obtain the PS Rocca's operator.

I present a review of the kinematics for PS-DMO. The impulse response is produced by taking an impulse on a constant offset section and migrating it to produce ellipses. Each element or point along the ellipses is then diffracted, setting offset to zero, to produce hyperbolas. This operation creates the impulse response that represents the Rocca's DMO+NMO operator (Claerbout, 1999).

Figure 1 shows a comparison between the Rocca's smear operator for single mode P data and for converted mode PS data. It is possible to observe, kinematically, that the Rocca's operator for converted waves is shifted laterally toward the receiver. This is the expected result, since the upgoing wave path is slower than the downgoing wave path.

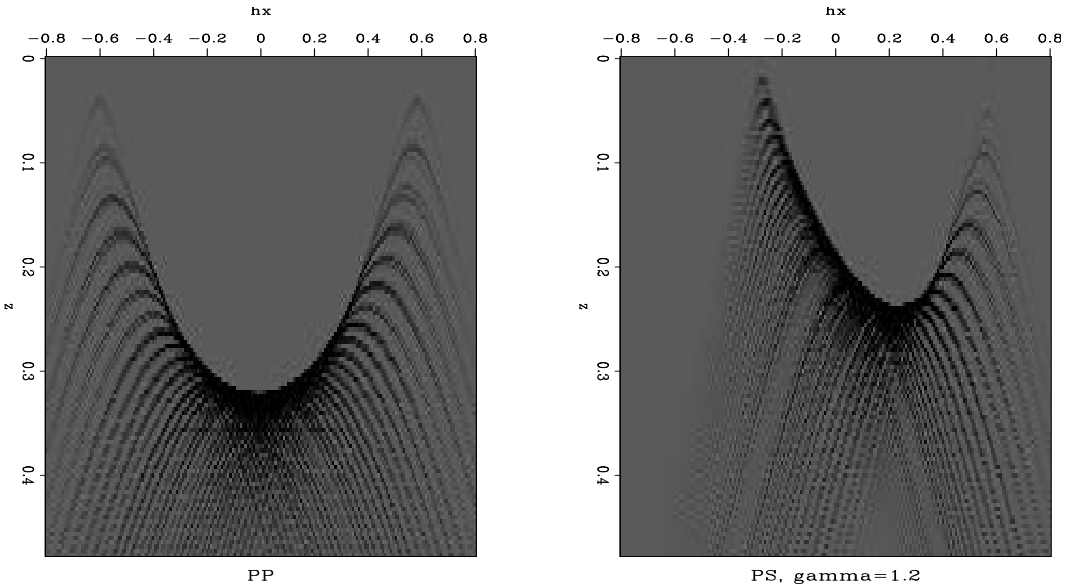

Figure 1: Rocca's operator, for single mode P data (left) and converted mode PS data (right) daniel2-rocca [ER,M]

Jaramillo (1997) shows the amplitude distribution for a PS-DMO operator. This amplitude distribution is also shown in Figure (1). The denser the dots, the higher the amplitude should be.

One of the challenges is to obtain an independent expression for the DMO operator, but

this task has already been solved in the literature. Here I present a review of this process, since the result is used by Rosales and Biondi (2002) and later in this paper.

PS-DMO smile derivation

The trajectory equation of conversion points is

$$t = \frac{\sqrt{z^2+(h+x)^2}}{v_p} + \frac{\sqrt{z^2+(h-x)^2}}{v_s}. \tag{1}$$

By introducing the ratio, $\gamma = \frac{v_p}{v_s}$, and by following Huub Den Rooijen's (1991) derivations, as well as work by Xu et al. (2001), we have the following standard form of elliptical equation:

$$z^2 + \left(1 - \frac{4\gamma h^2}{v_p^2 t^2}\right)(x+D)^2 = \frac{v_p t_n^2}{(1+\gamma)^2}, \tag{2}$$

where D is the element responsible for transforming the data from CMP coordinates to CCP coordinates. D comes from solving equation (1) for z^2. The difference among the existing PS-DMO operators is in their definition of D. In this paper we use the definition presented by Xu et al. (2001):

$$D = \left[1 + \frac{4\gamma h^2}{v_p^2 t_n^2 + 2\gamma(1-\gamma)h^2}\right]\frac{1-\gamma}{1+\gamma}h, \tag{3}$$

where t_n is the NMO-corrected time.

The spatial shift distance needed to convert CMP gathers to common-reflection point gathers is

$$b = x + z\frac{dz}{dx}. \tag{4}$$

The one-way normal-incidence distance R is given by

$$R^2 = z^2 + \left(z\frac{dz}{dx}\right)^2. \tag{5}$$

Using equations (2) and (4) we eliminate the z and x dependencies. This result is substituted in the relationship for the one-way normal-incidence distance R [equation (5)] in order to get the equation:

$$R^2 + (b+D)^2\left(\frac{v_p^2 t^2}{4\gamma h^2} - 1\right) = \frac{v_p^2 t_n^2}{(1+\gamma)^2}. \tag{6}$$

The two-way normal-incidence time is

$$t_0 = \frac{R}{v_p} + \frac{R}{v_s} = \frac{1+\gamma}{v_p}R, \tag{7}$$

and the traveltime equation, in terms of the normal moveout time, is

$$t^2 = t_n^2 + \frac{4\gamma h^2}{v_p^2}. \tag{8}$$

Combining equations (6), (7) and (8) produces the PS-DMO smile equation:

$$\frac{t_0^2}{t_n^2} + \frac{y^2}{H^2} = 1, \tag{9}$$

where

$$\begin{aligned} y &= x + D \\ H &= \frac{2\sqrt{\gamma}}{1+\gamma} h. \end{aligned}$$

PS-DMO IN THE FREQUENCY-WAVENUMBER LOG-STRETCH DOMAIN

The previous section shows a kinematic PS-DMO operator. Like PP-DMO, kinematic PS-DMO can not properly handle phase and amplitude (Xu et al., 2001). Xu et al. (2001); Alfaraj (1992) discuss a PS-DMO operator on the *f-k* domain by using a truncation of power series for the moveout of reflections from dipping reflectors in a constant velocity media.

Zhou et al. (1996) discuss that the PP-DMO operator in the *f-k* domain is computationally expensive because the operator is temporarily non-stationary. He uses the idea of Bolondi et al. (1982) to express a more accurate PP-DMO operator by a logarithmic time stretching.

Xu et al. (2001) exploit the idea of computational efficiency of the logarithmic time stretching for the PS-DMO operator, however their formulation is not clearly expressed. Therefore, I reformulate their work using the PS-DMO smile presented in the previous section and following a procedure similar to Hale (1984) and Zhou et al. (1996). This operation accounts for constant velocity case.

Starting from the PS wave DMO smile,

$$\frac{t_0^2}{t_n^2} + \frac{y^2}{H^2} = 1. \tag{10}$$

By following Hale's (1984) assumption that $p_0(t_0, x, H) = p_n(t_n, x, H)$, we obtain the 2D PS-DMO operator in the *f-k* domain:

$$P_0(\omega, k, H) = \int\int p_0(t_0, y, H) e^{i(\omega t_0 - ky)} dt_0 dy. \tag{11}$$

Equation (10) implies a change of variable from t_0 to t_n. Therefore, equation (11) becomes

$$P_0(\omega, k, H) = \int\int A^{-1} p_0(t_n, x, H) e^{i\omega A t_n} e^{-ik(x+D)} dt_n dx \tag{12}$$

where

$$A = \frac{dt_0}{dt_n} = \sqrt{1 + \frac{H^2 k^2}{t_n^2 \omega^2}}. \tag{13}$$

Equation (12) is the base for PS-DMO in the *f-k* domain. By using a time log-stretch transform pair,

$$\begin{aligned} \tau &= \log \frac{t}{t_c}, \\ t &= t_c e^{\tau}. \end{aligned} \tag{14}$$

The DMO operator in the *f-k* log-stretch domain becomes

$$P_0(\Omega, k, h) = P_n(\Omega, k, h) e^{ikD} F(\Omega, k, h), \tag{15}$$

where

$$F(\Omega, k, h) = e^{\frac{i}{2}\Omega \log \frac{1}{2}\left(\sqrt{\left(\frac{2kH}{\Omega}\right)^2 + 1} + 1\right)}. \tag{16}$$

When either kh or Ω gets the values of 0, the filter goes to 0 as well.

The previous expression is equivalent to the one presented by Xu et al. (2001). Note that equation (15) is based on the assumption that $p_0(t_0, x, H) = p_n(t_n, x, H)$. This doesn't include changes in midpoint position and/or common reflection point position. This allows for a correct kinematic operator but one with a poor amplitude distribution along the reflectors.

Zhou et al. (1996) refers to this problem in the log-stretch frequency wavenumber domain by reformulating Black's (1993) *f-k* DMO operator. This operator is based on the assumption that $p_0(t_0, x_0, H) = p_n(t_n, x_n, H)$. The midpoint location also changes, leading to a more accurate distribution of amplitudes. After implementing the PS-DMO operator Xu et al. (2001), extending this operator is a feasible task. Following the derivation used by Zhou et al. (1996), I state a more accurate PS-DMO operator in the log-stretch frequency wavenumber domain. This new operator differs from the previous one in the filter $F(\Omega, k, h)$. The new filter is

$$F(\Omega, k, h) = e^{\frac{i}{2}\Omega \left\{ \sqrt{1 + \left(\frac{2kH}{\Omega}\right)^2} - 1 - \log \frac{1}{2}\left[\sqrt{\left(\frac{2kH}{\Omega}\right)^2 + 1} + 1 \right] \right\}}. \tag{17}$$

This filter reduces to 0 if $kh = 0$ or kH if $\Omega = 0$.

Note that for a value of $\gamma = 1$, the filter reduces to the known expression for P waves data (Zhou et al., 1996).

Figure 2 shows a series of impulse responses for this operator in the frequency domain.

Figure 3 shows the same series of impulse responses as Figure 2 but with the new filter [equation (17)]. Both operators create the same kinematic response. However, Figure 3 shows that the filter in equation (17) gives a more accurate amplitude distribution along the impulse response.

We can trust the PS results since the PP impulse response, obtained with the filter in equation (17) and $\gamma = 1$, is the same as that obtained by Zhou et al. (1996). Moreover, the amplitude distribution follows Jaramillo's (1997) result.

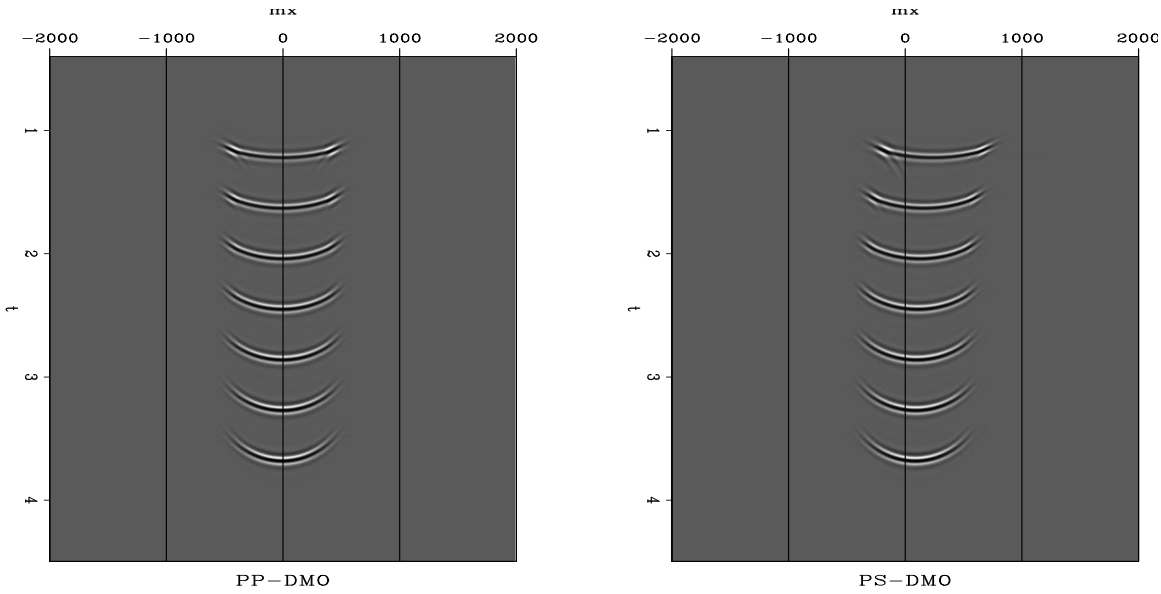

Figure 2: Impulse responses for the DMO operator, PP case (left), PS case (right) daniel2-imps [ER,M]

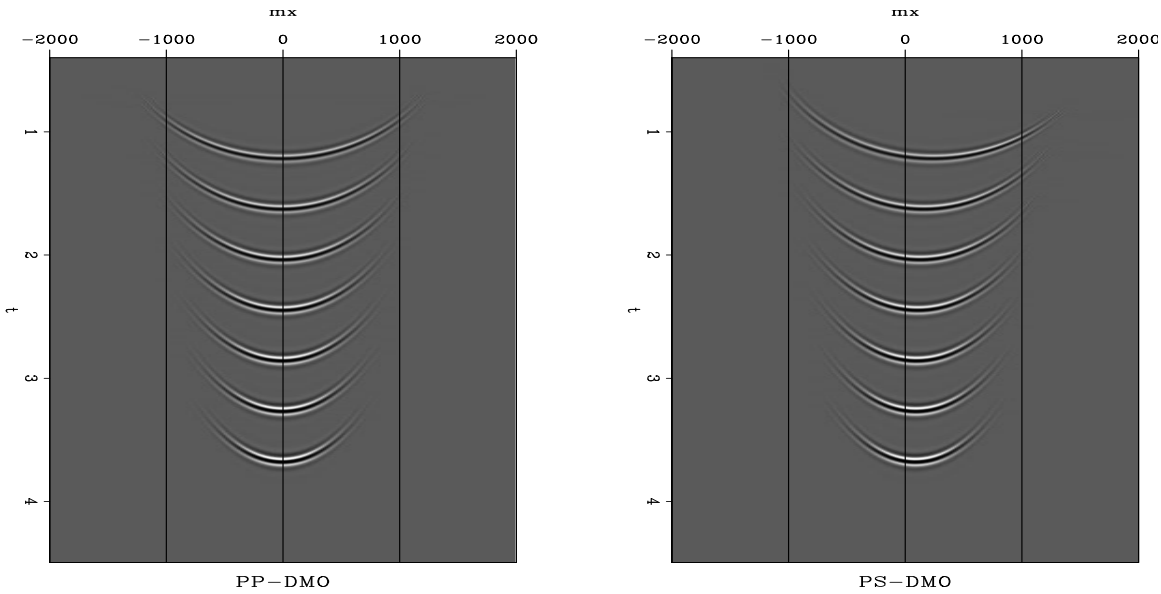

Figure 3: Impulse responses for the new PS-DMO operator, PP case (left), PS case (right) daniel2-imps-new [ER,M]

REAL DATA

In order to further test our operator, we apply it to a real data line. The Alba Oil Field is located in the UK North Sea and elongates along a NW-SE axis. The oil reservoir is 9km long, 1.5km wide, and up to 90m thick at a depth of 1,900m sub sea (**?**MacLeod et al., 1999).

The producing reservoir consists of unconsolidated high-porosity turbiditic sandstone of Eocene age. The oil-bearing reservoir sand and the overlying shale have a very low P-wave acoustic impedance contrast but make a significant S-wave velocity contrast. Hence, the reservoir delineation using only normal PP-seismic data is very difficult. Therefore, the ocean bottom PS-data was acquired (MacLeod et al., 1999).

Even though the Alba field is a 3D data set, we select one line by choosing a source line that overlaps a receiver line. There are several gaps in our selected data since we are taking a 2D line from a 3D data set.

Figure 4 shows a CMP gather from the PZ-component and the PS-component of the data. Note the gaps and irregularities in the data.

Figure 5 shows a comparison between the NMO stack and the DMO stack of the PP line. The DMO was performed by the same algorithm described here, specifying $\gamma = 1$.

Figure 6 shows the PS result. It compares the PS-NMO CCP binning stack and the PS-DMO stack. The PS-DMO stack was obtained using the filter described in equation (16). Observe that, even though it is a flat events area, those small dips are better defined after doing PS-DMO.

Figure 7 shows the PS-DMO result using the filter described in equation (17), which better handles the amplitudes. Note that some strong dip energy appears. The rest of the section remains the same. Therefore, the filter in equation (17) produces more accurate results.

DISCUSSION

The PS-DMO operator that we finally used is the operator in the *f-k* log-stretch domain. Since this operator is stationary in the time log-stretch domain, the use of FFT in both directions is possible. This makes the PS-DMO operator in the log-stretch frequency wavenumber domain a fast operator that yields accurate results.

This new operator is not only accurate kinematicly but also dynamicly becuase it includes CCP lateral position changes. This is a new result at the time this paper was written.

The operator is valid for constant velocity, however it is necessary to use the work done by other authors (Alfaraj, 1992; Hale, 1984) to incorporate depth variant velocity and depth variant γ.

The operator used here is safe, fast and valid for both PP and PS propagation modes. It is only necessary to specify a value of $\gamma = 1$ to obtain PP-DMO and an appropriate value of

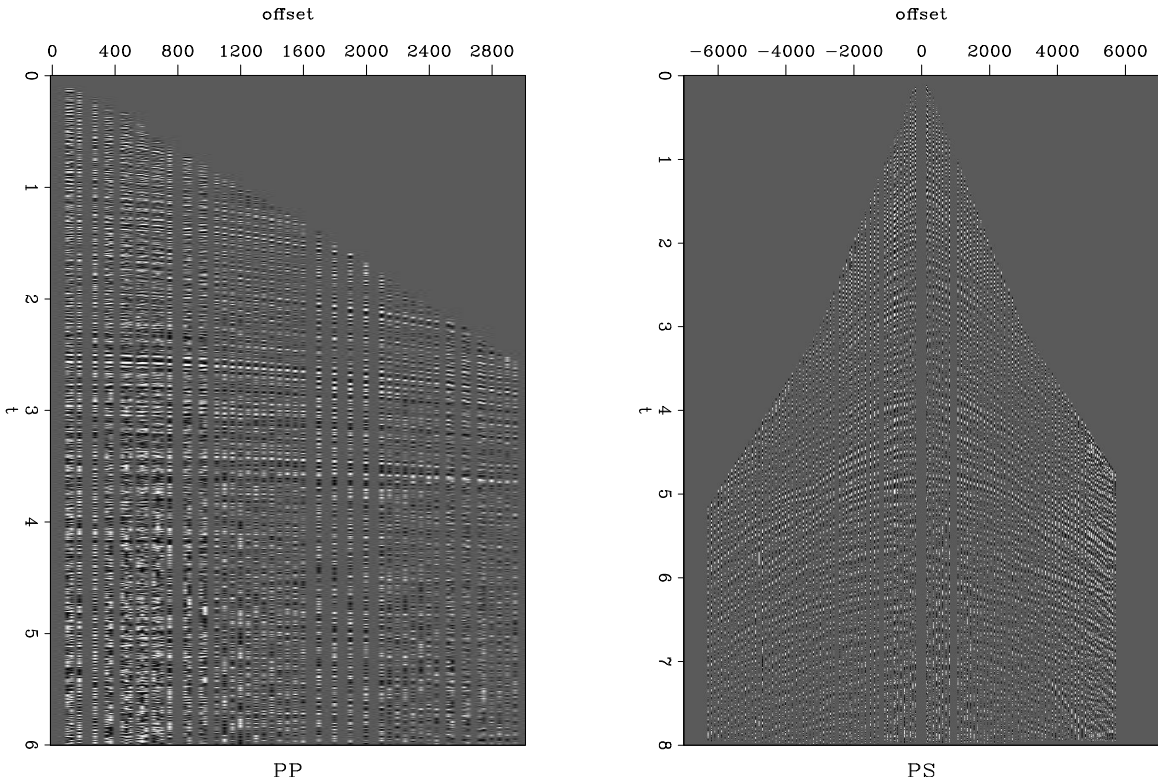

Figure 4: CMPS daniel2-cmps [ER]

$\gamma \neq 1$ and/or $\gamma > 1$ to obtain PS-DMO.

ACKNOWLEDGMENTS

I want to thank ChevronTexaco for providing the data set.

REFERENCES

Alfaraj, M., 1992, Transformation to zero offset for mode converted waves by Fourier transform: 62th Annual Internat. Mtg., Society Of Exploration Geophysicists, Expanded Abstracts, 974–977.

Black, J. L., Schleicher, K. L., and Zhang, L., 1993, True-amplitude imaging and dip moveout: Geophysics, **58**, 47–56.

Bolondi, G., Loinger, E., and Rocca, F., 1982, Offset continuation of seismic sections: Geophysical Prospecting, **30**, 813–828.

Claerbout, J. F., 1999, Basic earth imaging: Class notes, http://sepwww.stanford.edu/sep/prof/index.html.

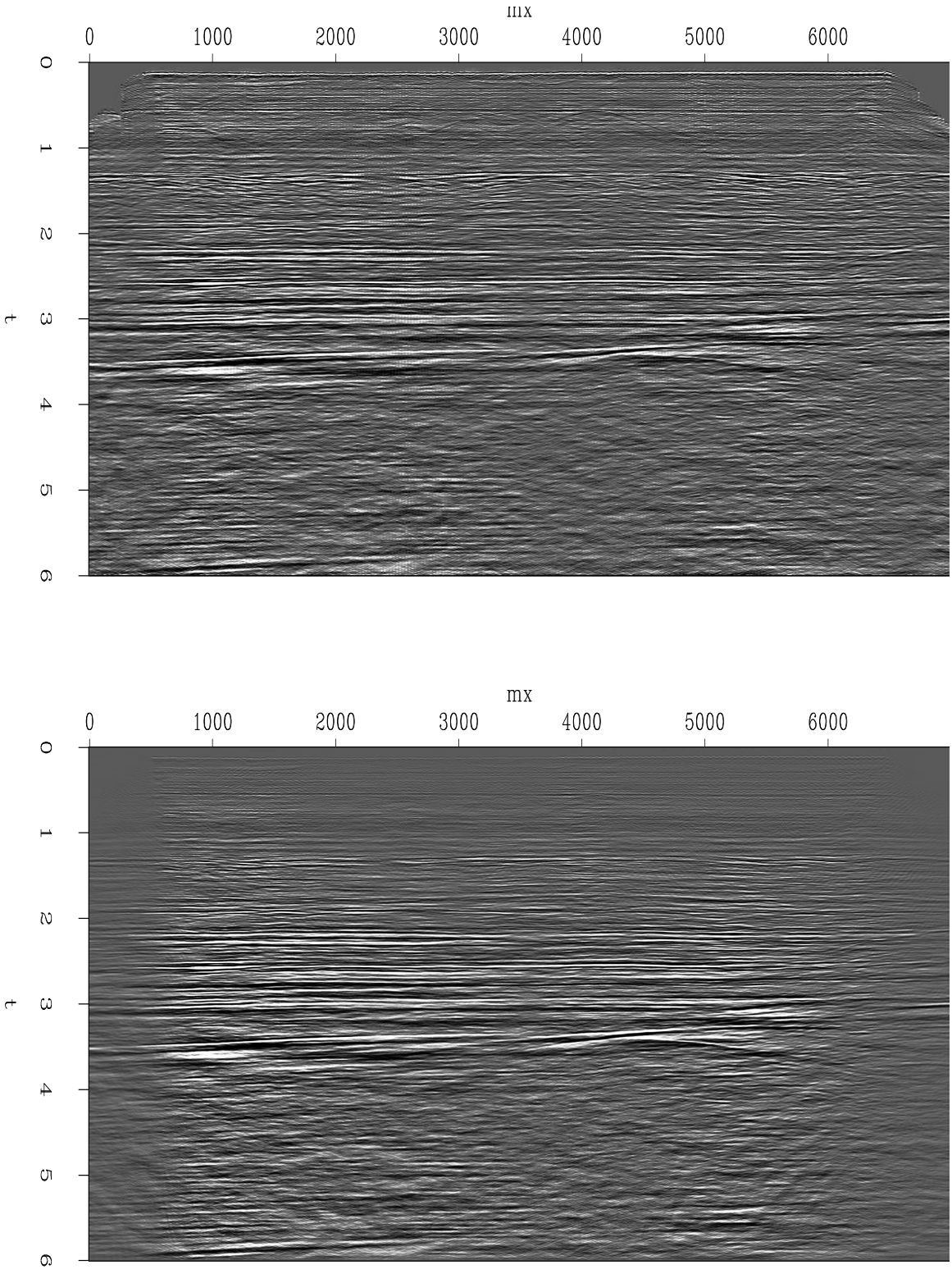

Figure 5: PP results, NMO-stack (top), DMO-stack (bottom) daniel2-pp [CR,M]

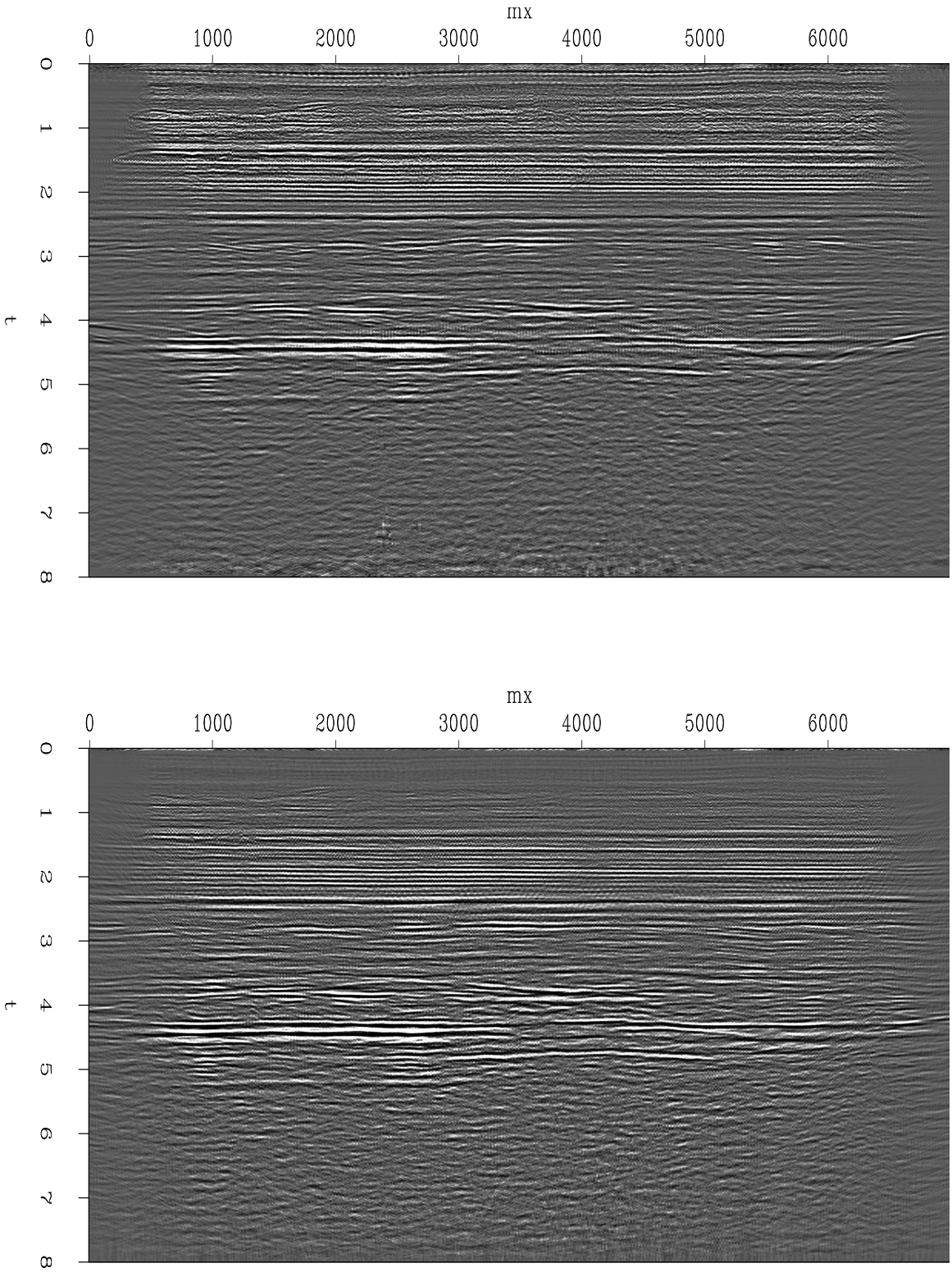

Figure 6: PS results, PS-NMO CCP binning stack (top), PS-DMO stack (bottom) daniel2-psone [CR,M]

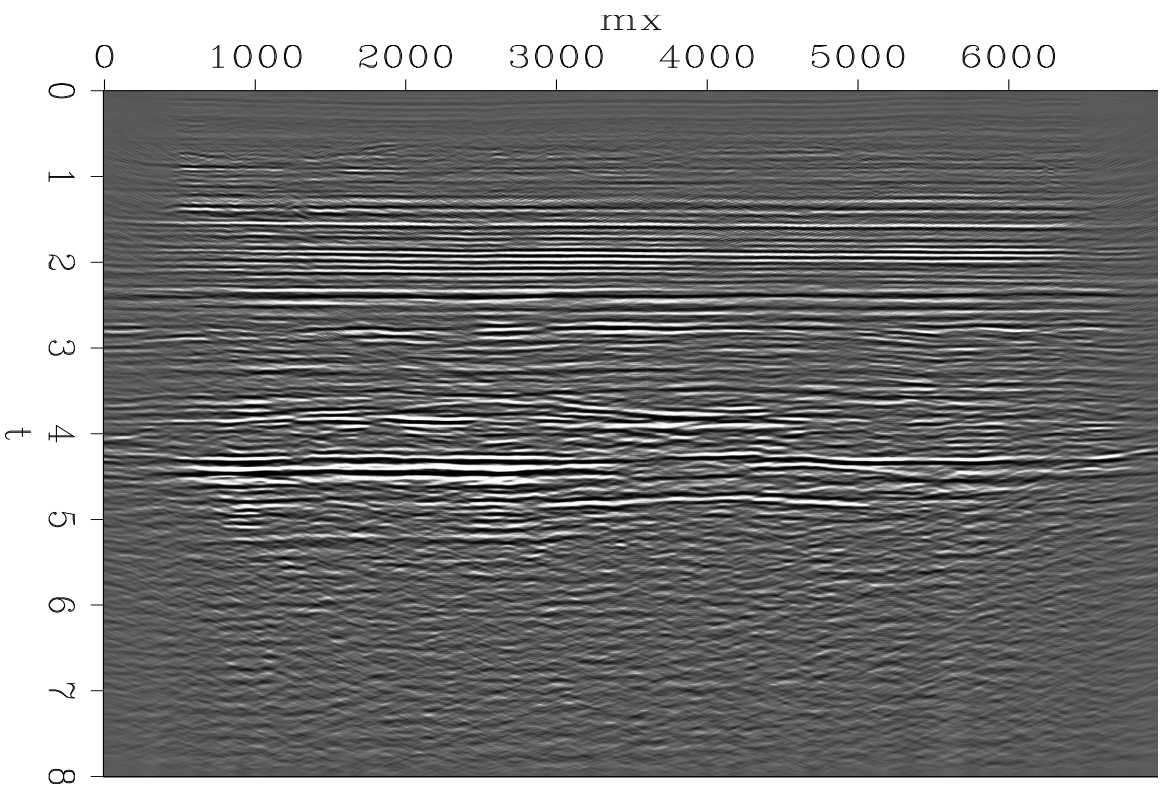

Figure 7: PS-DMO considering amplitudes daniel2-pstwo [CR,M]

Deregowski, S. M., and Rocca, F., 1981, Geometrical optics and wave theory of constant offset sections in layered media: Geophysical Prospecting, **29**, 384–406.

Hale, D., 1984, Dip moveout by Fourier transform: Geophysics, **49**, no. 6, 741–757.

Harrison, M., 1990, Converted wave DMO: 60th Annual Internat. Mtg., Society Of Exploration Geophysicists, Expanded Abstracts, 1370–1373.

Huub Den Rooijen, P. G. M., 1991, Stacking of P-SV seismic reflection data using dip moveout: Geophysical Prospecting, **39**, no. 4, 585–598.

Iverson, W. P., Fahmy, B. A., and Smithson, S. B., 1989, VpVs from mode-converted P-SV reflections: Geophysics, **54**, no. 7, 843–852.

Jaramillo, H. H., 1997, P-S converted-wave DMO in depth-variable velocity: 67th Annual Internat. Mtg., Society Of Exploration Geophysicists, Expanded Abstracts, 1594–1597.

MacLeod, M. K., Hanson, R. A., Bell, C. R., and McHugo, S., 1999, The Alba Field ocean bottom cable seismic survey: Impact on development: The Leading Edge, **19**, no. 11, 1306–1312.

Rosales, D., and Biondi, B., 2002, Converted wave azimuth moveout: SEP–**111**, 59–71.

Tessmer, G., and Behle, A., 1988, Common reflection point data-stacking technique for converted waves: Geophysical Prospecting, **36**, no. 5, 671–688.

Xu, S., Jin, S., Ma, Z., and Geng, J., 2001, A fast converted wave dip moveout in f-k domain: 71st Annual Internat. Mtg., Society Of Exploration Geophysicists, Expanded Abstract, 1851–1854.

Zhou, B., Mason, I. M., and Greenhalgh, S. A., 1996, An accurate formulation of log-stretch dip moveout in the frequency-wavenumber domain: Geophysics, **61**, no. 3, 17–23.